

# A Vertically Integrated CMOS Microsystem for Time-Resolved Fluorescence Analysis

Bruce R. Rae, *Member, IEEE*, Jingbin Yang, Jonathan McKendry, Zheng Gong, David Renshaw, John M. Girkin, Erdan Gu, Martin D. Dawson, *Fellow, IEEE*, and Robert K. Henderson, *Member, IEEE*

**Abstract**—We describe a two-chip micro-scale time-resolved fluorescence analyzer integrating excitation, detection, and filtering. A new  $8 \times 8$  array of drivers realized in standard low-voltage  $0.35\text{-}\mu\text{m}$  complementary metal–oxide semiconductor is bump-bonded to AlInGaN blue micro-pixelated light-emitting diodes (micro-LEDs). The array is capable of producing sample excitation pulses with a width of 777 ps (FWHM), enabling short lifetime fluorophores to be investigated. The fluorescence emission is detected by a second, vertically-opposed  $16 \times 4$  array of single-photon avalanche diodes (SPADs) fabricated in  $0.35\text{-}\mu\text{m}$  high-voltage CMOS technology with in-pixel time-gated photon counting circuitry. Captured chip data are transferred to a PC for further processing, including histogramming, lifetime extraction, calibration and background/noise compensation. This constitutes the smallest reported solid-state microsystem for fluorescence decay analysis, replacing lasers, photomultiplier tubes, bulk optics, and discrete electronics. The system is demonstrated with measurements of fluorescent colloidal quantum dot and Rhodamine samples.

**Index Terms**—Biophotonics, biosensors, complementary metal–oxide semiconductor (CMOS) integrated circuits (ICs), fluorescence, fluorescence lifetime, GaN micro-light-emitting diodes, single-photon avalanche diodes.

## I. INTRODUCTION

QUANTITATIVE fluorescence intensity measurements are often prone to misinterpretation. Typical sources of error include fluorophore concentration variation, photo-bleaching, excitation light nonuniformity, and the presence of other factors which may result in emission quenching or enhancement. In addition, background light and autofluorescence can distort quantitative intensity-based measurements [1]. Thus, there is a growing interest in time-resolved fluorescence detection, where the characteristic fluorescence decay time constant (or lifetime) in response to an impulse excitation source is measured. Furthermore, fluorophores can be designed so that their lifetime properties are sensitive to the conditions

Manuscript received May 12, 2010; revised August 10, 2010; accepted September 06, 2010. Date of current version November 24, 2010. This work was supported by the UK Engineering and Physical Sciences Research Council under the “HYPIX” program. This paper was recommended by Associate Editor G. Yuan.

B. R. Rae, J. Yang, D. Renshaw, and R. K. Henderson are with the Joint Research Institute for Integrated Systems, Institute for Micro and Nano Systems, School of Engineering, The University of Edinburgh, Edinburgh, EH9 3JL, U.K. (e-mail: Bruce.Rae@ed.ac.uk).

J. McKendry, Z. Gong, E. Gu, and M. D. Dawson are with the Institute of Photonics, University of Strathclyde, Glasgow, G4 0NW, U.K.

J. M. Girkin is with the Department of Physics, Durham University, Durham, DH1 3LE, U.K.

Color versions of one or more of the figures in this paper are available online at <http://ieeexplore.ieee.org>.

Digital Object Identifier 10.1109/TBCAS.2010.2077290

within their local microenvironment, such as pH and oxygen levels, and this provides an extremely powerful analysis tool.

Conventional equipment required to perform fluorescence lifetime analysis is bulky and expensive. Typical setups include a picosecond pulsed or modulated light source (often a laser source); a sensitive detector, such as a microchannel plate photomultiplier tube (MCP-PMT); an optical system, frequently incorporating a microscope for low-volume measurements, as well as a variety of optical lenses and filters. Optical lab-on-a-chip (LoC) applications for point-of-care diagnostics equipment are now motivating research into the miniaturization of fluorescence lifetime instrumentation.

Complementary metal–oxide semiconductor (CMOS)-compatible detectors offer the opportunity to produce highly integrated fluorescence detection systems capable of monolithic detector data processing, at low cost. Recent developments in the design of CMOS-compatible single-photon avalanche diodes [2] allow extremely sensitive detectors to be integrated alongside signal-processing circuitry. In order to gather photon arrival time data, from which fluorescence lifetimes can be extracted, a number of circuit techniques have been proposed. These include on-chip time-to-digital converters [3], in-pixel time-gated counters [4], and pinned photodiodes [5].

A truly miniaturized optical LoC requires miniature and low-cost excitation sources as well as detectors. Several fluorescence lifetime detector arrays have now been demonstrated in CMOS [3]–[5]. However, the aspect of miniaturized excitation sources has been largely neglected, relying on pulsed lasers with expensive and bulky drive electronics.

Micro-LED devices have recently been demonstrated to produce subnanosecond pulses suitable for lifetime analysis [6], where the excitation of a fluorescence sample was demonstrated using external LED drivers and a PMT detector.

In addition to the hardware requirements of time-resolved fluorescence analysis, there are also significant computational demands associated with the extraction of lifetime values from captured data. This often involves the postprocessing of data in order to fit exponential decay curves, from which lifetime estimations can be obtained. In order to provide rapid lifetime estimations for point-of-care or real-time applications, a number of algorithms have been proposed [7], [8]. These algorithms allow lifetime values to be obtained quickly and can be used to provide feedback on experimental dynamics during the period of observation, without the need for data postprocessing.

In this paper, we combine a dedicated CMOS-driven micro-LED chip with a second CMOS SPAD array in a two-chip “sandwich” structure (Fig. 1). Incorporating an excitation source with a photodetector, on-chip driving electronics,

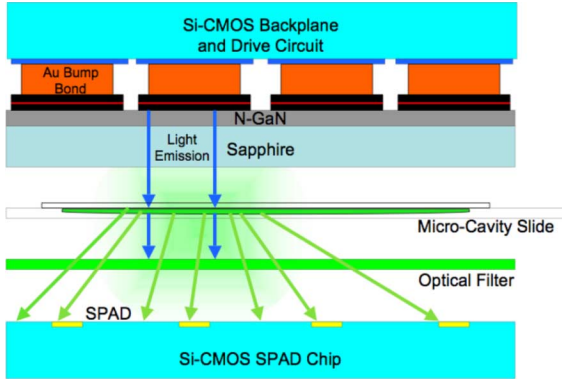


Fig. 1. Cross-section of the two-chip microsystem. The sample of interest is introduced in a microcavity slide sealed by a cover slip. An optical filter prevents excitation light from reaching the detector array.

and lifetime signal-processing circuitry, our devices represent a highly integrated LoC system [9]. A number of intensity-based fluorescence-sensing microsystems have recently been reported [10]–[12]; however, to the best of our knowledge, this is the first CMOS-based microsystem designed specifically for time-resolved fluorescence measurements. By including much of the signal processing and timing on-chip, the input/output (I/O) requirements and jitter sensitivity of the system are greatly reduced. The pixellation of detector and emitter arrays eases alignment constraints, reduces sample photobleaching, and provides multiplexed analysis capability. With the addition of micro-optics, the pixelated excitation and detection devices have the potential to act as a 2-D sensor array. Currently, however, the system operates as a single-point lifetime sensor through the binning of pixel outputs. To the best of our knowledge, the 777-ps optical pulsewidth is the shortest reported pulse for a CMOS-driven micro-LED device, emitting at 450 nm. GaN-based light sources have peak emission in the ultraviolet (UV)/blue/green region of the visible light spectrum. The micro-LED wavelength was chosen to be 450 nm since this provides a close match with the excitation wavelength of many commonly used fluorophores. The inclusion of a 514-nm-long pass optical filter allows excitation and fluorescence photons to be separated, due to the Stoke’s shift phenomenon, thus reducing measurement error. As a description of the system hardware, details of supporting software developments are provided. This includes a description of a software-implemented fluorescence lifetime extraction algorithm and histogramming tool along with a background as well as dark-count calibration methods and a system calibration technique. The accurate detection of commonly used, short lifetime fluorophores (Rhodamine 6G and Rhodamine B, with maximum emissions at 555 nm and 583 nm, respectively [13]) and longer lifetime CdSe/ZnS colloidal semiconductor quantum dots (emission peak at 520 nm [14]) are presented down to nanomolar concentration.

## II. DEVICE IMPLEMENTATION

### A. Excitation Array

Sample excitation is achieved using an  $8 \times 8$  array of  $72\text{-}\mu\text{m}$  diameter, AlInGaN blue micro-pixelated light-emitting diodes (micro-LEDs) that are fabricated from “standard” InGaN/GaN

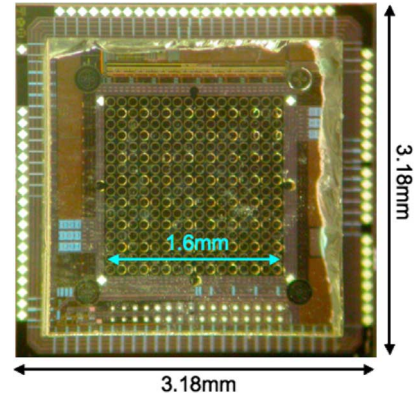


Fig. 2. AllInGaN micro-LED array bump-bonded to an  $8 \times 8$  CMOS driver array.

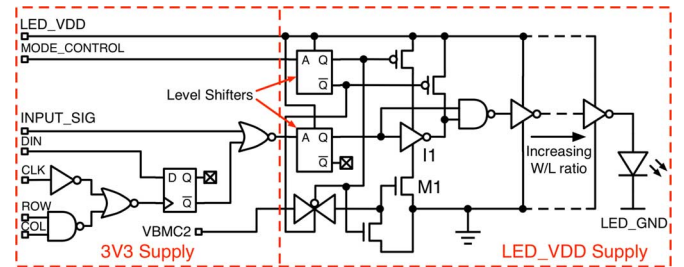


Fig. 3. CMOS driver element, illustrating the output buffer and short-pulse generation circuitry.

quantum well blue LED wafers (planer n- and p-type GaN layers), grown on *c*-plane sapphire substrates by metal organic chemical vapor deposition [15]. This micro-LED array is bump-bonded to an equivalent array of LED driver circuits realized in standard low-voltage  $0.35\text{-}\mu\text{m}$  CMOS technology (Fig. 2). Each array element (or pixel) is individually addressable, with a dedicated driver circuit per micro-LED. An  $8 \times 8$  array, with a  $200\text{-}\mu\text{m}$  pitch was chosen to allow a  $100\text{-}\mu\text{m}$  bond stack to be implanted within each pixel, compatible with the available bump-bonding process. However, scaling to  $20\text{-}\mu\text{m}$  diameter devices within  $128 \times 96$  arrays has been demonstrated in [16]. The wavelength spectra of the CMOS-driven blue micro-LED device peaks at a wavelength of 450 nm.

The CMOS driver array pixels measure  $200\text{ }\mu\text{m} \times 200\text{ }\mu\text{m}$ , at the  $200\text{-}\mu\text{m}$  pitch. Each pixel contains a dedicated driver circuit, driving a full metal bond-stack to which the micro-LED is bump-bonded (Fig. 3). All driver input signals were based on 3.3-V logic before being level-shifted to a higher user-definable voltage ( $LED\_VDD$ ), to a maximum of 5 V. Adjusting  $LED\_VDD$  allows the user to tune the LED intensity and, therefore, photon count rates can be controlled in order to avoid pulse pileup effects. This allows standard 3.3-V logic to be used for the addressing and control circuitry in the pixel before the signal level is increased to  $LED\_VDD$  (requiring the use of physically larger transistors, due to a thicker gate oxide, to be able to withstand 5 V).

The driver circuit is capable of producing optical pulses of user-definable width variable from 47.48 ns down to 777 ps, FWHM ( $\pm 180\text{-ps}$  estimated measurement error, based on PMT RMS jitter), Fig. 4. By placing a square-wave signal

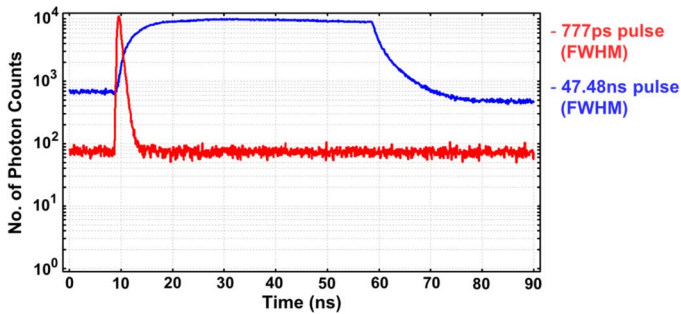


Fig. 4. Shortest and longest micro-LED excitation pulses.

TABLE I  
SUMMARY OF THE MICRO-LED DRIVER ARRAY

Performance	
Array Size	8x8
Driver Pitch	200 $\mu$ m
Shortest Optical Pulse	777ps
Excitation Wavelength	450nm
Max. Voltage	5V
Max. Driver Current	236mA (DC)
VCO Frequency Range	7MHz-800MHz
Die Size	3.18x3.18mm <sup>2</sup>

on *INPUT\_SIG*, the delay through inverter I1 defines the pulsewidth. The inverter delay can be adjusted via the gate voltage (*V<sub>BMC2</sub>*) of the current-starving NMOS transistor M1. The level-shifted dc, pulsed, or square-wave signal is then passed through an output buffer designed using 5-V transistors. To minimize load capacitance on the input signal while maximizing the drive strength of the circuit, an output buffer comprising a chain of inverters of increasing transistor width/length ratios has been implemented.

An on-chip voltage-controlled oscillator (VCO) has also been implemented within the 8  $\times$  8 driver array. Comprised of a current-starved ring oscillator, this circuit is capable of producing a square-wave signal with a tunable frequency range from 7 to 800 MHz. The VCO output can be used as the input signal to the drivers of the main array, defining the frequency of a square-wave or pulsed input signal. By producing a square-wave input signal on-chip, the need for an off-chip clock (such as a crystal oscillator) has been removed, potentially reducing system size and cost. The performance of the micro-LED excitation array is summarized in Table I.

### B. Detection Array

Our SPAD detector array is the same as that reported in [17] now combined with the separate emitter chip described in this paper. It consists of a 16  $\times$  4, 200- $\mu$ m pitch array of SPAD detectors implemented in a 0.35- $\mu$ m high-voltage CMOS process. The pixels contain a 28.27- $\mu$ m<sup>2</sup> active area SPAD structure as reported in [18] biased in Geiger mode at  $-19.5$  V via a passive quench PMOS transistor. Sensitive down to a single photon, the SPAD output pulses can either be buffered off-chip via an inverter circuit located locally within the SPAD pixel for processing by external photon counting hardware, or processed locally within each pixel by time-gated ripple counters (Fig. 5). SPAD pulses provide the asynchronous clock to the first T-type flip-flop in the counter. A ripple counter was chosen

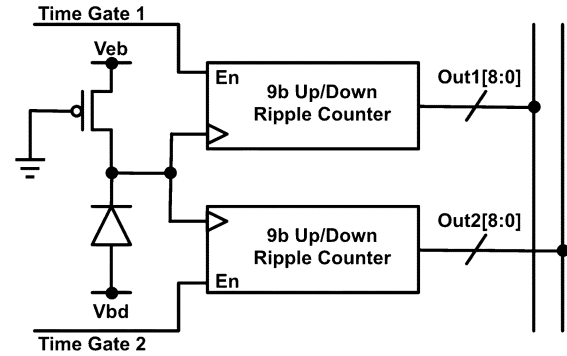


Fig. 5. SPAD circuit with passive quench transistor and two associated 9b ripple counters.

to minimize the clock loading, since no synchronous count behavior is required. Time-gated operation is accomplished by providing the toggle input of the first T-type flip-flop in the counter with short pulses, which are generated within the pixel from delayed versions of the system phase-locked-loop (PLL) output. During time-gate periods, the counters are enabled and count the number of SPAD output pulses. Out with this time-gate period, any SPAD output pulses are ignored by the counter circuit. These counters allow histogram and lifetime analysis without the need for external photon counting hardware and significantly reduce the quantity of data required to be broadcast off-chip.

Synchronization of the time-gated detection circuit and the micro-LED excitation array is achieved by using the VCO circuit located on the LED driver chip as the input to the timing generator circuit situated on the SPAD chip. This circuit defines the positions of the time gate and consists of a 120-element tapped delay line composed of current-limited buffers. Each delayed output can be selected independently under the control of a latched shift register. In this way, the time gate is inherently synchronized with the excitation pulse, reducing errors due to uncorrelated timing jitter.

### C. System Configuration

Fig. 6 shows the configuration of the two-chip system. A dedicated daughter card was designed, with the micro-LED device situated on the underside of the printed-circuit board (PCB), facing the SPAD detector chip located on the main PCB test board. Electrical connection to the daughter card is made via stacked header pins.

This technique allows the distance between the micro-LED device and the SPAD detector chip to be adjusted. Both devices share the same core power supplies and ground connections. These supplies and all other bias supplies, apart from the negative SPAD bias, are generated on the test board PCB and derived from the 5-V supply of the USB2.0 connection. The negative SPAD supply is generated by an external power source. The devices share a single field-programmable gate array (FPGA) situated on an Xilinx experimentation module PCB (Opal Kelly, XEM3010), which generates the digital input signals to both devices.

The excitation and detection arrays have a minimum separation of 3 mm (to allow the sample to be placed between the two devices). However, in order to accommodate an optical filter and

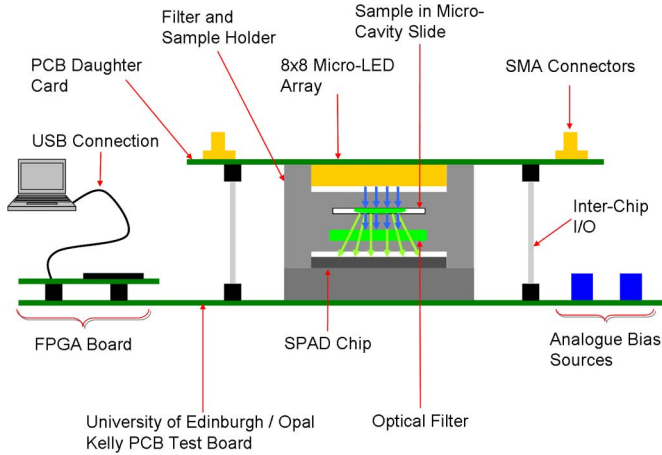


Fig. 6. Complete two-chip microsystem. The PCB daughter card is physically supported by the filter and sample holder and stacked header pins.

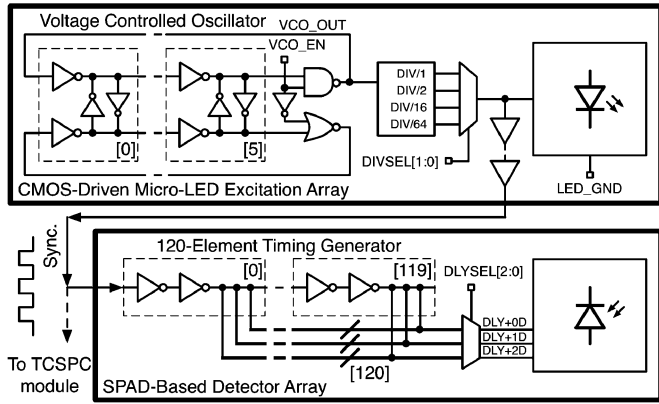


Fig. 7. On-chip VCO provides the square-wave input to the micro-LED driver array and the SPAD time-gate generator circuit.

the sample of interest, a device separation of 1 cm was used to obtain the results reported herein. A plastic holder was designed to house these two elements, providing a light tight enclosure for the packaged SPAD chip, an optical filter, a sample held in a microcavity slide and a packaged micro-LED device.

The frequency of the LED device is defined by the output from the on-chip VCO, situated on the micro-LED driver chip. This signal is passed off-chip and is used as the synchronization input to either a time-correlated single photon counting (TCSPC) module (Becker and Hickl, SPC-130), or the timing generator circuit on-board the detector chip (Fig. 7). The synchronization of the two devices when operating in on-chip time-gated photon counting mode is described by the timing diagram in Fig. 8.

A 514-nm long-pass filter (Semrock, LP02-514RU-25) was chosen to separate the excitation light from the fluorescence emission. This allows a range of fluorophores with emission spectra greater than 514 nm to be evaluated while maximizing the rejection of excitation light. A photograph of the complete two-chip microsystem can be seen in Fig. 9.

### III. DEVICE OPERATION

The unit delay of the on-chip signal delay generator is sensitive to process, voltage, and temperature variation. Inaccuracy

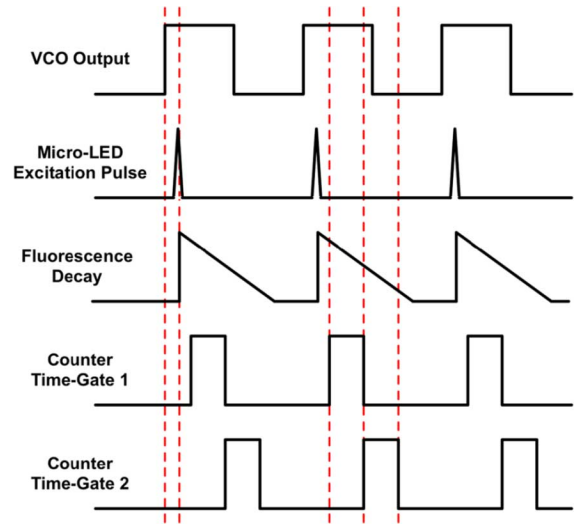


Fig. 8. Timing for synchronization of the VCO, micro-LED excitation pulses, and SPAD chip time gates.

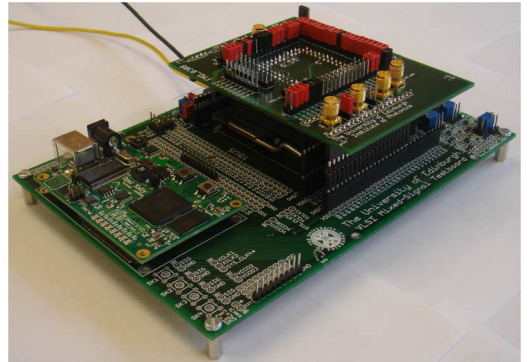


Fig. 9. Complete two-chip microsystem.

in the time-gate width can lead to error in any lifetime estimations made. Therefore a calibration step is essential to calculate the actual value of the unit delay. This is achieved using the micro-LED device as a reference. Using a PLL clock from the FPGA test board, a micro-LED element is pulsed at a known frequency. With no fluorescent sample present, the SPAD array is then used to count photons from this LED pulse stream. Using the on-chip gated counters, a time gate of minimum width is swept across the full delay range of the timing generator. When the position of the time gate is coincident with the micro-LED pulse, a sharp increase in photon counts is obtained. The frequency of the PLL clock is then shifted by a known amount and the process is repeated. This is summarized in Fig. 10.

By counting the number of time bins between the peaks of these two micro-LED pulses ( $N$ ) while noting the change in PLL frequency, the time difference between the two peaks can be calculated using (1). Dividing this by  $N$  allows the width of an individual time bin to be calculated

$$\text{delay\_time} = \frac{1}{f_1} - \frac{1}{f_2}, \quad (f_2 > f_1) \quad (1)$$

$$\text{unit\_delay} = \frac{\frac{1}{f_1} - \frac{1}{f_2}}{N}, \quad (f_2 > f_1) \quad (2)$$

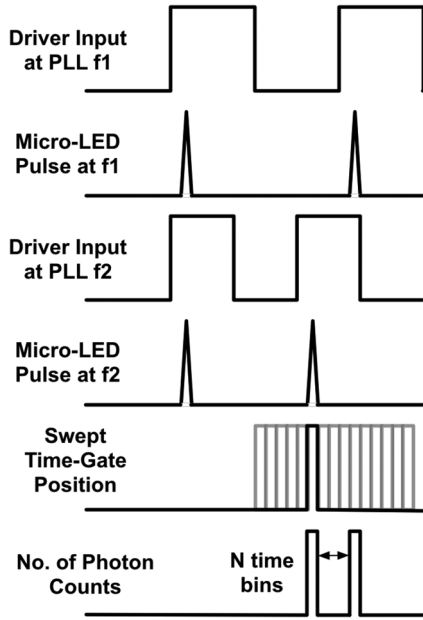


Fig. 10. Time-gate width calibration.

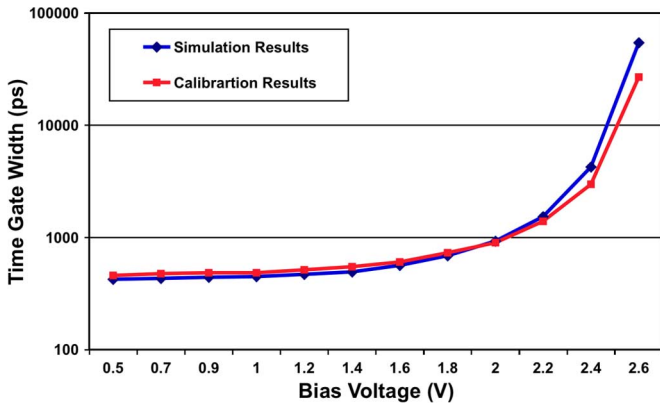


Fig. 11. Simulation results and calibration measurements of time gate width under different bias voltages.

where  $f_1$  and  $f_2$  are the micro-LED pulse frequencies at times 1 and 2, respectively. As described in [15], the time-gate width is user definable and can be controlled by varying the gate bias voltage of current-starving transistors within the delay generator. Fig. 11 shows how the gate width varies with bias voltage and how this variation is tracked by the calibration procedure.

This calibration step is performed at the start of an experimental procedure. The measured time-gate width is stored by the software and is subsequently used during the lifetime estimation process.

In order to provide the user with information on the dark-count profile of the detector array, the system software allows the user to generate a dark-count map. Performed in a dark environment and using a fixed exposure time, each SPAD detector address is visited and a dark-count measurement is performed. Fig. 12 shows a typical profile of dark-count across the array, which is in line with the previously reported results [19]. The exposure time used for this measurement was 1 min. Using this data, a threshold can be set in the software, allowing

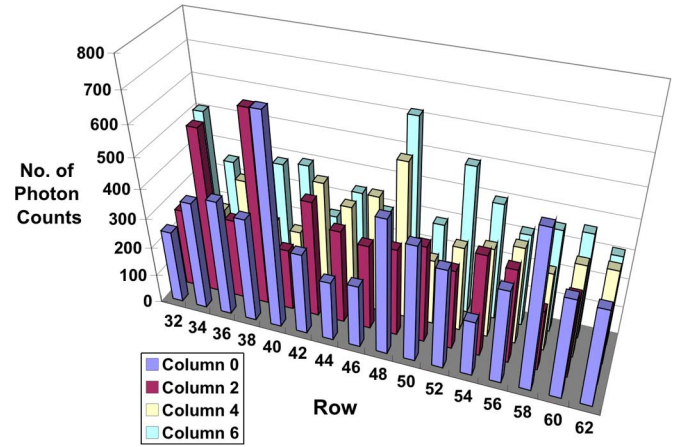


Fig. 12. Histogram of dark count values, acquired over a 60-s time period, across array.

high dark-count SPADs to be ignored during the measurement process.

In order to quickly provide the system user with fluorescence lifetime estimations of a single exponential decay from the on-chip time-gated photon counting, an extraction algorithm has been employed. The algorithm chosen for this system is the two-gate rapid-lifetime-determination algorithm (2-RLD, (3)) [8]

$$\tau = \frac{\Delta T}{\ln\left(\frac{TG1}{TG2}\right)} \quad (3)$$

where  $\tau$  is the lifetime of the fluorophore,  $\Delta T$  is the time difference between the start of the two time gates, and  $TG1$  and  $TG2$  are the number of counts gathered in the first and second time gates, respectively. The two in-pixel counters allow photons from the two different time-gate periods to be collected simultaneously, improving photon efficiency and, thus, reducing measurement times and sample exposure to potentially harmful excitation light. This algorithm has been implemented in software and provides the user with instantaneous lifetime estimations without the need to postprocess histogram data. In order to speed up experiment times or improve lifetime estimations by enhancing the number of photon counts per time gate, the output of several pixels can be summed prior to lifetime estimation.

The original algorithm was modified to allow measurement data to be adjusted to compensate for system noise due to background light and detector darkcounts. In order to achieve this, an additional measurement step was undertaken in order to establish system noise levels prior to sample excitation (Fig. 13).

The modified 2-RLD algorithm with noise compensation is shown as

$$\text{Lifetime} = \frac{\Delta T}{\ln\left(\frac{N1-N0}{N2-N0}\right)} \quad (4)$$

where  $N0$  is the number of background counts captured prior to sample excitation.

Without noise compensation, the ratio of  $N1$  over  $N2$  becomes small, resulting in lifetime estimations which are shorter than the actual value. The width of the time-gate  $N0$  must be the same as that used for  $N1$  and  $N2$ . By subtracting the number of counts in  $N0$  from those in  $N1$  and  $N2$ , the residual counts

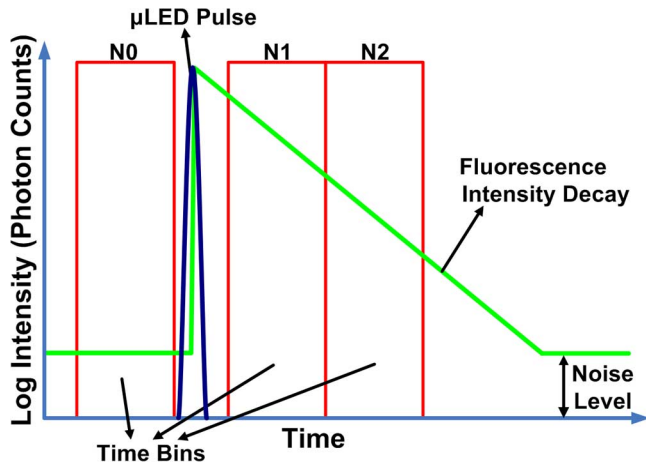


Fig. 13. The 2-RLD technique with noise compensation. A time gate, N0, before the micro-LED pulse is required to gather background/noise data.

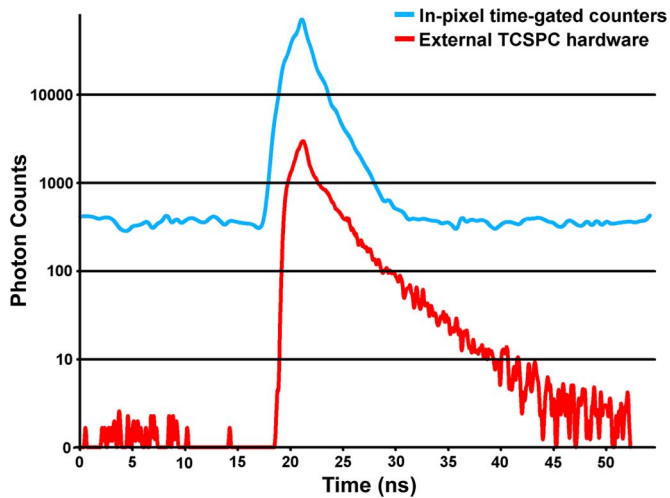


Fig. 14. Fluorescence decay of Rhodamine 6G, captured by using in-pixel time-gated counters and external TCSPC hardware.

can be attributed to fluorescence. This process improves the accuracy of the estimate lifetime.

In order to allow the user to observe a fluorescence decay or instrument response function, while still making use of the lifetime extraction algorithm, the software was configured to allow histogram data to be displayed. By sweeping a time gate of minimum width ( $\sim 450$  ps) across the full range of the on-chip timing generator, data from each time-point can be gathered and a histogram can be generated. Fig. 14 shows the decay curve of a Rhodamine 6G sample, captured by using both histogrammed in-pixel counter data and external TCSPC hardware.

#### IV. RESULTS

In order to establish the sensitivity of the SPAD detector and on-chip time-gating circuitry, a dilution experiment was performed where different concentrations of CdSe/ZnS quantum dot samples (Evident Technologies Inc.) diluted in toluene were analyzed (Fig. 15). The SPAD detector was mounted to the output port of a microscope (Nikon, TE2000-U) and the sample excited by a 470-nm picosecond pulsed laser diode (PicoQuant, GmbH). It was found that the SPAD detector and in-pixel time-

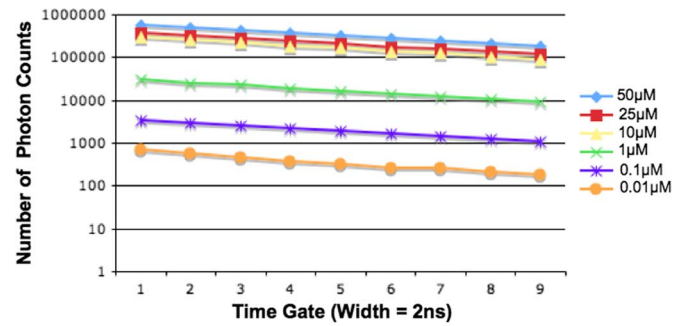


Fig. 15. Fluorescence decay curves of quantum dot samples at different concentrations, captured using the SPAD detector and in-pixel time-gated counters.

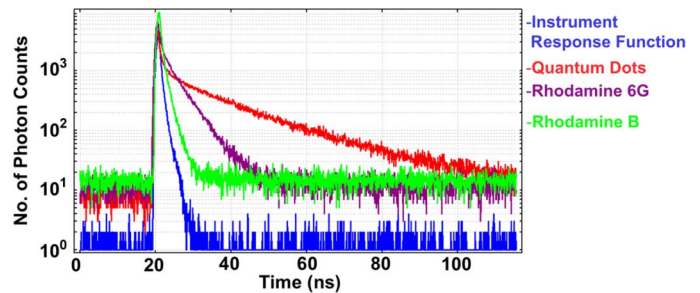


Fig. 16. Fluorescence decay curves of quantum dot, Rhodamine 6G and Rhodamine B samples. An IRF of 910-ps FWHM is also included.

gated counters were capable of performing time-resolved analysis of these samples down to a concentration of 10 nM. From these decay curves, lifetimes of 13.7, 13.7, 13.5, 13.8, 13.1, and 13.4 ns ( $\pm 408$ -ps estimated measurement error, based on the timing generator circuit resolution) were extracted for sample concentrations of 50, 25, 10, 1, 0.1, and 0.01  $\mu\text{M}$ , respectively. These results are competitive with those quoted in the literature for CMOS-based sensors intended for time-resolved fluorescence. In [3], results are obtained using a sample of 1-mM concentration, and in [20] concentrations from 32 nM down to 320 pM are used although no lifetime values have been extracted from the results.

Measurements of fluorescence decay curves using the two-chip microsystem and external TCSPC hardware were obtained using quantum dots in a toluene solution (concentration = 57  $\mu\text{M}$ ) and Rhodamine 6G (concentration = 250  $\mu\text{M}$ ) and Rhodamine B (concentration = 100  $\mu\text{M}$ ) in water (Fig. 16). An analysis of these decay curves yields lifetime estimations of 13.8 ns, 4.3 ns, and 1.3 ns for the quantum dot sample, Rhodamine 6G and Rhodamine B samples, respectively ( $\pm 80$ -ps estimated measurement error, based on SPAD rms jitter). These results were performed with an LED excitation pulsewidth of 910 ps (FWHM), using a sample volume of 45  $\mu\text{L}$ , and are consistent with lifetimes reported in [13] and [14]. Furthermore, quantum dot lifetimes are consistent with those measured using a conventional microscope system, confirming the ability of the microsystem to accurately resolve fluorescence lifetime data.

In order to verify the performance of the software-embedded 2-RLD algorithm, a series of tests was performed using a 250- $\mu\text{M}$  Rhodamine 6G sample. A mean lifetime of 3.6 ns was

estimated. This measurement was repeated a number of times with lifetime values varying by just 3.31%. These lifetime estimations were compared to measurements conducted using a commercially available, external TCSPC setup (Becker & Hickl, SPC-130), where a lifetime of 3.7 ns was estimated with a variation of 2.33%. These results demonstrate the devices' ability to provide the user with accurate lifetime estimations quickly and without the need for any data postprocessing.

## V. CONCLUSION

A compact fluorescence lifetime analysis system based on scalable and potential low-cost technologies (CMOS, GaN), along with conventional electronic components (FPGA, PCB), has been demonstrated. The presented results show the accurate detection of commonly used fluorophores at practical concentration levels. Using a rapid-lifetime determination algorithm, featuring dark-count and ambient light correction, lifetime estimation can be obtained quickly. This paper opens up the possibility of a low-cost, robust, and potentially portable diagnostic or sensing system, capable of detecting changes in analytes with lifetime properties sensitive to specific biological, chemical, or environmental factors. Future work includes addressing the mismatch in the format of the detection and excitation arrays as well as scaling both devices (implemented test structures incorporating  $30\ \mu\text{m} \times 30\ \mu\text{m}$  bond-stacks have successfully been bump-bonded to micro-LED devices). In addition, we intend to investigate the removal of the optical filter to further reduce device dimensions [21] and the incorporation of microfluidics as a sample delivery method.

## ACKNOWLEDGMENT

The authors would like to thank Optocap Ltd., U.K., for carrying out the bump-bonding process, Prof. Charbon at TU Delft for access to the SPAD devices and K. Muir at The University of Edinburgh for his assistance. They would also like to thank the Scottish Funding Council for the Scottish Consortium on Integrated Microphotonic Systems (SCIMPS) for their support along with the the Joint Research Institute with Heriot-Watt University, which is a part of the Edinburgh Research Partnership in Engineering and Mathematics (ERPem).

## REFERENCES

- [1] J. R. Lakowicz and K. W. Berndt, "Lifetime-selective fluorescence imaging using and rf phase-sensitive camera," *Rev. Sci. Instrum.*, vol. 62, no. 7, pp. 1727–1734, 1991.
- [2] A. Rochas, M. Gani, B. Furrer, P. A. Besse, and R. S. Popovic, "Single photon detector fabricated in a complementary metal-oxide-semiconductor high-voltage technology," *Rev. Sci. Instrum.*, vol. 74, p. 3263, 2003.
- [3] D. E. Schwartz, E. Charbon, and K. L. Shepard, "A single-photon avalanche diode array for fluorescence lifetime imaging microscopy," *IEEE J. Solid-State Circuits*, vol. 43, no. 11, pp. 2546–2557, Nov. 2008.
- [4] D. Mosconi, D. Stoppa, L. Pancheri, L. Gonzo, and A. Simoni, "CMOS single-photon avalanche diode array for time-resolved fluorescence detection," in *Proc. Eur. Solid-State Circuits Conf.*, 2006, pp. 564–567.
- [5] H. J. Yoon, S. Itoh, and S. Kawahito, "A CMOS image sensor with in-pixel two-stage charge transfer for fluorescence lifetime imaging," *IEEE Trans. Electron Devices*, vol. 56, no. 2, pp. 214–221, Feb. 2009.

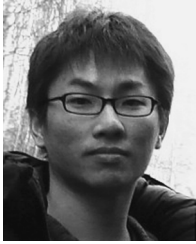
- [6] C. Griffin, E. Gu, H. Choi, C. Jeon, O. Rolinski, D. Birch, J. Girkin, and M. Dawson, "Fluorescence excitation and lifetime measurements using GaN/InGaN micro-led arrays," in *Proc. IEEE 17th Annu. Meeting Lasers and Electro-Optics Soc.*, Nov. 2004, vol. 2, pp. 896–897.
- [7] D. Li, J. Arlt, J. Richardson, R. Walker, A. Buts, D. Stoppa, E. Charbon, and R. Henderson, "Real-time fluorescence lifetime imaging system with a  $32 \times 32$   $0.13\ \mu\text{m}$  CMOS low dark-count single-photon avalanche diode array," *Opt. Expr.*, vol. 18, no. 10, pp. 10257–10269, 2010.
- [8] H. C. Gerritsen, M. Asselbergs, A. V. Agronskaia, and W. Van Sark, "Fluorescence lifetime imaging in scanning microscopes: Acquisition speed, photon economy and lifetime resolution," *J. Microscopy*, vol. 206, pt. 3, pp. 218–224, June 2002.
- [9] J. A. Chediak, Z. Luo, J. Seo, N. Cheung, L. P. Lee, and T. D. Sands, "Heterogeneous integration of CdS filters with GaN LEDs for fluorescence detection microsystems," *Sens. Actuators A, Phys.*, vol. 111, pp. 1–7, 2004.
- [10] N. Nelson, D. Sander, M. Dandin, A. Sarje, S. Prakash, J. Honghao, and P. Abshire, "A handheld fluorometer for measuring cellular metabolism," in *Proc. IEEE Int. Symp. Circuits and Systems*, 2008, pp. 1080–1083.
- [11] R. R. Singh, D. Ho, A. Nilchi, G. Gulak, P. Yau, and R. Genov, "A CMOS/thin-film fluorescence contact imaging microsystem for DNA analysis," *IEEE Trans. Circuits Syst. I, Reg. Papers*, vol. 57, no. 5, pp. 1029–1038, May 2010.
- [12] B. Jang, P. Cao, A. Chevalier, A. Ellington, and A. Hassibi, "A CMOS fluorescent-based biosensor microarray," in *Proc. IEEE Int. Solid-State Circuits Conf.*, 2009, pp. 436–437, 437a.
- [13] ISS, Lifetime data of selected fluorophores. [Online]. Available: <http://www.iss.com/resources/fluorophores.html>
- [14] Evident Technologies, EviDot specifications. [Online]. Available: <http://www.evidenttech.com/products/evidots/evidot-specifications.html>
- [15] C. Jeon, H. Choi, E. Gu, and M. Dawson, "High-density matrix-addressable AlInGaN-based 368-nm microarray light-emitting diodes," *IEEE Photon. Technol. Lett.*, vol. 16, no. 11, pp. 2421–2423, Nov. 2004.
- [16] H. W. Choi, C. W. Jeon, and M. D. Dawson, "Fabrication of matrix-addressable micro-LED arrays based on a novel etch technique," *J. Cryst. Growth*, vol. 268, no. 3–4, pp. 527–530, 2004.
- [17] B. R. Rae, C. Griffin, K. R. Muir, J. M. Girkin, E. Gu, D. Renshaw, E. Charbon, M. D. Dawson, and R. K. Henderson, "A microsystem for time-resolved fluorescence analysis using CMOS single-photon avalanche diodes and micro-LEDs," in *Proc. Int. Solid-State Circuits Conf.*, 2008, pp. 166–167.
- [18] C. Niclass, M. Sergio, and E. Charbon, "A single photon avalanche diode array fabricated in deep-submicron CMOS technology," in *Proc. Design, Automation and Test in Eur.*, 2006, vol. 1, pp. 1–6, 6–10.
- [19] E. Charbon, "Towards large scale CMOS single-photon detector arrays for lab-on-chip applications," *J. Phys. D: Appl. Phys.*, vol. 41, no. 9, 2008.
- [20] F. Borghetti, D. Mosconi, L. Pancheri, and D. Stoppa, "A CMOS single-photon avalanche diode sensor for fluorescence lifetime imaging," in *Proc. Int. Image Sensor Workshop*, 2007, pp. 250–253.
- [21] D. Stoppa, D. Mosconi, L. Pancheri, and L. Gonzo, "Single-photon avalanche diode CMOS sensor for time-resolved fluorescence measurements," *IEEE Sensors J.*, vol. 9, no. 9, pp. 1084–1090, Sep. 2009.



**Bruce R. Rae** (M'08) was born in Aberdeen, U.K., in 1983. He received the M.Eng. and Ph.D. degrees in electrical and electronic engineering from The University of Edinburgh, Edinburgh, U.K., in 2005 and 2009, respectively.

While working toward his M.Eng. degree, he was with ST Microelectronics' Imaging Division. His Ph.D. project focused on the design and implementation of a low-cost, miniaturised complementary metal-oxide semiconductor (CMOS)-based microsystem for time-resolved fluorescence analysis.

Since 2008, he has been a Postdoctoral Research Associate at the Institute for Integrated Micro and Nanosystems which is part of The University of Edinburgh, School of Engineering. His research interests include the design of CMOS-based systems for fluorescence lifetime analysis, single-photon counting, and control circuitry for micro-light-emitting-diode devices.



**Jingbin Yang** was born in Shenzhen, China, in 1986. He received the two-year B.Sc. degree in information engineering at South China University of Technology in 2005 and 2006, and the M.Eng. (Hons.) degree in electronics and electrical engineering from the University of Edinburgh, Edinburgh, U.K.

Then, he received the Sir William Siemens Medal from Siemens Ltd. in 2009. During his M.Eng. project, he demonstrated a fully automated lifetime extraction microsystem. He has a keen interest in mixed-signal analog-digital circuitry.



**Jonathan McKendry** received the M.Eng. degree in electronics and electrical engineering from the University of Glasgow, Glasgow, U.K.

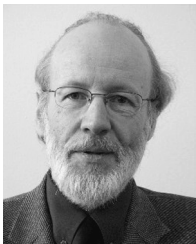
His Ph.D. project focuses on the development of optical biochips for use in applications, such as the analysis of complex DNA samples. His research deals with areas, including the integration of micro-light-emitting diode arrays with complementary metal-oxide semiconductor control circuitry and single-photon avalanche diode detectors to perform functions, such as fluorescence lifetime

imaging microscopy and visible light communications. He joined the Institute of Photonics, University of Strathclyde, Glasgow, in 2007.



**Zheng Gong** received the Ph.D. degree in condensed matter physics from the Institute of Semiconductors, Chinese Academy of Sciences (CAS), Beijing, China, in 2005, where he mainly focused on the molecular-beam-epitaxy growth and characterization of low-dimensional semiconductor quantum structures, such as In(Ga)As/GaAs quantum wires, quantum dots, and quantum rings.

He received a Liuyonglin Special Award from the Circuits and Systems Society in 2005. Since 2005, he has been a Research Fellow with the Institute of Photonics, University of Strathclyde, Glasgow, U.K., becoming involved in the fabrication, characterization, and application of GaN-based light-emitting diodes.



**David Renshaw** received the B.Sc. degree in pure mathematics, the M.Sc. degree in electronics, and the Ph.D. degree in very large-scale integration (VLSI) design from the University of Edinburgh, Edinburgh, U.K.

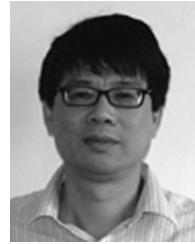
In 1989, a small research team under his direction designed and demonstrated the first single-chip complementary metal-oxide semiconductor (CMOS) video camera. In 1990, he was one of three founding members of VLSI Vision Ltd. (VVL), where he was a Technical Manager from 1990 to 1995. During that period, VVL grew from a research idea to 80 employees, became the leading supplier of CMOS imager chips and was placed on the London Stock Market. In 1996, he resumed teaching and academic research in the areas of CMOS image sensors, image-sensor processors, image-processing applications, and CMOS mixed analog-digital circuits.

Dr. Renshaw retired from full-time teaching in 2009 and is currently an Honorary Lecturer at the School of Engineering and Electronics, The University of Edinburgh.



**John M. Girkin** is the Chair in Biophysics at Durham University, Durham, U.K., having previously been with the Institute of Photonics, Strathclyde University, Glasgow U.K., and with commercial companies. He is also Co-Director of the Biophysical Sciences Institute at Durham University, with the aim of bringing physical science methodology to help with grand biological challenges. His interest is in the development and application of novel photonics-based technologies to help answer major questions presented in the life sciences. His

research stretches from advanced optical microscopy to the development of novel dental-imaging systems for clinical applications and desktop genotyping devices.



**Erdan Gu** received the Ph.D. degree in thin-film physics from Aberdeen University, Aberdeen, U.K., in 1992.

Currently, he is an Associate Director and Research Team Leader at the Institute of Photonics, University of Strathclyde, Glasgow, U.K., where he has been since 2002. Then, he was appointed Research Fellow at Cavendish Laboratory, Cambridge University, U.K. In 1997, he joined the thin-film research group, Oxford Instruments plc, U.K. as a Senior Research Scientist. At the Institute of

Photonics, he is responsible for a range of research activities and projects, such as micro/nano photonics and optics, micro/nano light-emitting diode device development and applications, diamond optics and photonics, and hybrid organic/inorganic optoelectronic devices. In these research fields, he has published many papers in international leading journals.



**Martin D. Dawson** (M'85-SM'98-F'09) received the B.Sc. and Ph.D. degrees in physics from Imperial College London, London, U.K.

Currently, he is Professor and Director of Research at the Institute of Photonics, University of Strathclyde, where he has been since 1996. He has almost 30 years of research experience gained in academia and industry in the U.S. and U.K. He leads a group with wide-ranging interests in GaN optoelectronics, hybrid GaN/polymer photonics, diamond photonics, and semiconductor disk lasers.

Prof. Dawson is a Fellow of the Optical Society of America, Institute of Physics, and Royal Society of Edinburgh.



**Robert K. Henderson** (M'89) received the Ph.D. degree from the University of Glasgow, Glasgow, U.K., in 1990.

Currently, he is a Senior Lecturer at the School of Engineering in the Institute for Microelectronics and Nanosystems, University of Edinburgh, Edinburgh, U.K. Since 1991, he has been a Research Engineer at the Swiss Centre for Microelectronics, Neuchatel, Switzerland, working on low-power sigma-delta analog-to-digital converters and digital-to-analog converters for portable electronic systems. In 1996,

he was appointed Senior VLSI Engineer at VLSI Vision Ltd., Edinburgh, where he worked on the world's first single-chip video camera and was Project Leader for many other complementary metal-oxide semiconductor (CMOS) image sensors. Since 2000, as Principal VLSI Engineer in the ST Microelectronics Imaging Division, he led the design of the first image sensors for mobile phones, resulting in annual revenues of several hundred million dollars. He joined the University of Edinburgh in 2005 to pursue his research interests in CMOS integrated-circuit design, imaging, and biosensors. As PI on the joint European project MegaFrame with three European Universities and ST Microelectronics, he has led research resulting in the first single-photon avalanche diode (SPAD) in nanometer CMOS technology. He is the author of many papers and 15 patents.

Dr. Henderson was awarded the Best Paper Award at the 1996 European Solid-State Circuits Conference as well as the 1990 IEE J. J. Thomson Premium.